JOURNAL OF MATERIALS SCIENCE 26 (1991) 82–92

A study of the influence of fibre/resin adhesion on the mechanical behaviour of ultra-high-modulus polyethylene fibre composites

B. TISSINGTON, G. POLLARD*, I. M. WARD
*IRC in Polymer Science and Technology and *School of Materials, University of Leeds, Leeds LS2 9JT, UK*

The interlaminar shear strength of unidirectional ultra-high-modulus polyethylene composites was measured as a means of accessing the level of fibre/epoxy resin adhesion for a number of different reinforcing yarns, produced by melt and gel-spinning. The fibres were shown to possess poor adhesive properties due partly to inadequate wetting associated with the inert polyolefine surface and also because of a weak boundary layer, formed by the segregation of low molecular weight impurities to the surface during fibre formation. The interlaminar shear strength was significantly increased by pretreating the reinforcement with an oxygen plasma. This improved wetting by producing oxygen-containing groups on the fibre surface and removed the weak boundary layer by the formation of a cross-linked skin. For a fixed fibre volume fraction, the interlaminar shear strength was found to be inversely proportional to the filament diameter. The other mechanical properties were shown to be largely independent of fibre/resin adhesion, with plasma treatment having little or no effect.

1. Introduction

During the last few years, ultra-high-modulus polyethylene (UHMPE) fibres have been developed using both melt-spinning and gel-spinning followed by drawing at high temperature to very high draw ratios [1, 2]. These fibres are gradually finding applications in composite materials, where their advantage in terms of high ductility, chemical stability and transparency to high-frequency radiation can be utilized to advantage.

It was recognized at an early stage of the development of the melt-spun and drawn fibres that their chemical inertness, whilst an asset in some respects, also makes for surface properties likely to ensure poor adhesion between the fibres and conventional matrices. Previous studies at Leeds University [3, 4], showed that plasma etching in an oxygen atmosphere could lead to significant improvements in fibre/resin adhesion. The present investigation extends the previous research in two major respects. Firstly, it examines in more detail the nature of the polymer surface following plasma treatment, and shows that part of the improvement in adhesion can be attributed to the removal of a weak boundary layer at the surface due to cross-linking arising during plasma treatment. Secondly, it includes comparative studies of composites containing high-modulus polyethylene fibres produced by alternative routes, including gel-spinning.

2. Experimental procedure

2.1. Materials

Four UHMPE yarns were examined.

(i) Celanese (Celanese Research, New Jersey, USA) melt-spun from linear polyethylene ($M_w = 60\,000$, $M_n = 20\,000$). The fibres were then drawn to a draw ratio of 30:1 following the principles described previously in the scientific and patent literature [5, 6].

(ii) Snia (Snia Fibre, Milan, Italy) also melt-spun but from a polyethylene of different molecular weight ($M_w = 170\,000$, $M_n = 17\,000$) and drawn to a 30:1 draw ratio.

(iii) Tekmilon (Mitsui Petrochemicals Ltd, Tokyo, Japan) produced by a modified melt-spinning process [7], in which a low molecular weight wax was added to the melt. The fibres were spun from an intermediate molecular weight polyethylene ($M_w = 700\,000$, $M_n = 50\,000$) and then drawn to a ratio of 50:1 at 130 °C using *n*-decane as a heat medium.

(iv) Spectra 1000 (Allied Corporation, New Jersey, USA) produced by the gel-spinning and drawing process [2], using a high molecular weight polyethylene ($M_w = 1\,500\,000$). The final filament draw ratio was 40:1.

Polyethylene monofilament was produced by melt-spinning a linear polyethylene (Unifos-2912) with $M_w = 224\,000$ and $M_n = 24\,100$. This was then drawn in a glycerol bath at 120 °C to a draw ratio of 30:1, giving a filament diameter of $\sim 70\,\mu m$. Glycerol was removed by washing in warm water and drying in an oven at 60 °C for 6 h.

The resin used in the fabrication of the composites was Araldite LY 1927/GB (Ciba-Geigy). This is a low-viscosity resin intended for use in high-strength composites.

0022–2461/91 $03.00 + .12

2.2. Treatment of reinforcement

In order to improve adhesion between the polyethylene fibres and resin matrix, the reinforcement was exposed to an oxygen plasma. Plasma treatment was performed using the Plasmaprep 300 unit, manufactured by Nanotech Ltd, Manchester, UK. This has a 300 W, 13.56 MHz radiofrequency power supply, with a capacitively coupled electrode discharge. The cylindrical reaction chamber is 30 cm long with a diameter of 15 cm. The carrier gas is blown along its axis.

Bundles of fibres were suspended along the length of the reaction chamber, attached to a glass frame. Using oxygen as the plasma carrier gas, the conditions of treatment were power 120 W, gas flow rate 17 $cm^3 min^{-1}$, pressure 0.4 torr*, duration 120 sec. These conditions were chosen so as to produce the full benefits of plasma treatment in a reasonably short time, while the bulk properties of the yarn were unaffected.

2.3. Preparation of composites

All the samples used in these tests were unidirectional composites, produced using the leaky die technique [3]. This uses a two-part, open-ended mould, which is capable of producing five composite bars at a time. These have a length of 200 mm and an approximate width of 10 mm.

The mould was initially coated with a release agent. A small amount of resin was then poured into each slot, on to which bundles of yarn were laid. The remaining resin was then added until the fibres were soaked. The upper section of the mould was then placed in position and a load of 25 kg applied, the excess resin flowing from the open ends.

The resin was cured for 16 h at room temperature, followed by 5 h at 50 °C. The fibre volume fraction was approximately 0.55.

2.4. Mechanical testing of composites

All measurements were performed on an Instron tensile testing machine.

2.4.1. Flexural tests

The flexural properties of the composites were measured in three-point bending, the direction of reinforcement lying perpendicular to the loading and support rods. The basic test data are given in Table I.

The interlaminar shear strength (ILSS) was determined using a short-beam bending rig, the geometry of which is designed to cause the composites to fail in shear at the fibre/resin interface [8]. This therefore provides an effective method of determining the level of adhesion between the two components. The ILSS is given by the expression

$$\text{ILSS} = 3P/4bd \quad (1)$$

where P is the failure load, b is the width and d is the thickness of the sample.

The deformation of UHMPE composites in three-point bending showed linearity only at low strains. It was therefore necessary to determine the flexural modulus at very small deflections, equivalent to about 0.08% maximum tensile strain. The FM value of each sample was determined by averaging the results from three bending cycles, calculated using the formula

$$\text{FM} = mL^3/4bd^3 \quad (2)$$

where m corresponds to the slope of the load–displacement plot, taken from the chart recorder, and L is the span between the supporting rods.

The ultimate flexural strength (UFS) was determined by simply measuring the maximum load achieved during bending. The UFS is given by

$$\text{UFS} = 3PL/2bd^2 \quad (3)$$

2.4.2. Tensile tests

The specification for the tensile strength (TS) and tensile modulus (TM) measurements are given in Table I. In both cases it was necessary for the ends of each sample to be sandwiched between soft aluminium plates (10 mm × 60 mm), using a cold-setting epoxy adhesive. This reduced the problems of stress transfer between the composite sample and the Instron grips.

For the TS measurements the samples were waisted to a continuous radius of 1 m on their broad face not, as is more usual, on the width. This meant that there was no parallel gauge length.

The TM samples were unwaisted. Strain was measured using an extensometer attached to the sample via spring-loaded knives. An initial preload of 80 kg was applied, intended to ensure that each sample was completely straight. A test load of 100 kg was then applied in four cycles of loading and unloading. The TM was calculated by averaging the last three cycles as the first often showed irregularities.

2.4.3. Compressive strength

The compressive strength (CS) tests were performed using equipment specially designed to avoid buckling, shown schematically in Fig. 1. The sample is gripped at each end by conically shaped clamps. The sample/clamp assembly is placed inside a steel tube, preventing any lateral movement. This arrangement results in a very short gauge length. The compressive load is applied using an Instron and the sample details are included in Table I.

2.5. Mechanical tests on yarn

The tensile strength and initial modulus of each of the multifilament yarns were also measured using an Instron testing machine (Table II). The ends of the yarn were gripped between 0.5 mm thick sheets of polyethylene, in order to avoid damage from the clamp faces. Applying a slight twist and damping with water allowed a more even distribution of stress between the

* 1 torr = 133.322 Pa.

TABLE I Specifications for mechanical testing

Test	Rod diameter(mm)		Gauge length (mm)	Width (mm)	Thickness (mm)	Cross-head speed (mm min^{-1})
	Supporting	Loading				
ILSS	6.0	6.0	10	10	2.1	2.0
UFS	10.0	20.0	80	10	2.1	20
FM	10.0	20.0	160	10	2.1	10
TM	–	–	25	10	2.1	0.3
TS	–	–	Thickness waisted to a continuous 1m radius	10	~ 1	5.0
CS	–	–	10	10	2.1	1.0

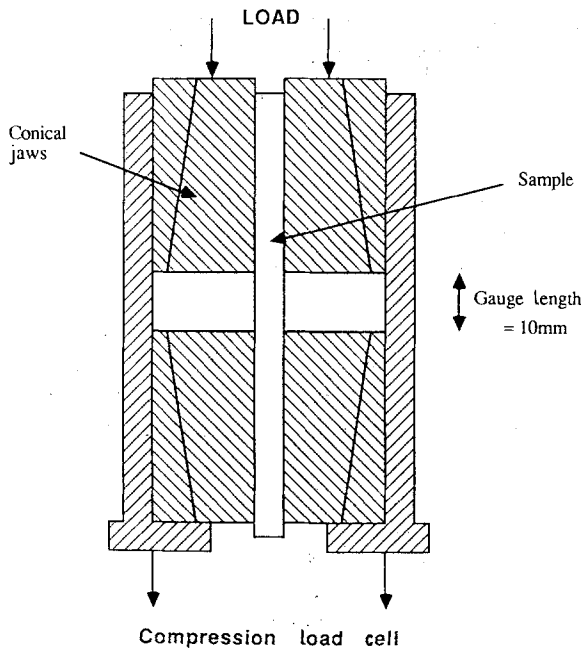

Figure 1 Schematic representation of the compression rig.

TABLE II Mechanical properties of yarn

	Tensile strength (GPa)	Tensile modulus (GPa)	Extension to failure (%)
Celanese	0.8	43	8
Snia	1.2	58	6
Spectra	2.3	83	4
Tekmilon	1.8	70	5

filaments. The fibres were deformed at a rate of 20% min^{-1}, with a gauge length of 200 mm.

2.6. Scanning electron microscopy

Scanning electron microscopy (SEM) was performed with a Hitachi S700 using accelerating voltages of 5 to 10 kV. Low voltages were needed in order to avoid electron-beam damage of the samples.

The specimens were first coated using an Edwards Sputter Coater S150B, with a water-cooling system. To avoid excessive heating and thermal degradation of the polymer, coating was performed continuously for no longer than 2 min, the required thickness being built up in a series of layers (typically five).

For some examinations, the UHMPE reinforcement was removed from the composites by refluxing in xylene for 10 min. The sample was then washed in acetone and the process repeated, followed by drying in an air oven at 40 °C for 1 h. This treatment was used in an attempt to expose a replica of the fibre surface in the resin matrix.

2.7. Filament diameter

The filament diameter of each yarn was measured using a calibrated eye piece on an optical microscope, at a magnification of X400.

2.8. Gel content

The degree of cross-linking produced by plasma treatment was determined in accordance with the American National Standard D2765. A weighed quantity of material was placed in a stainless steel gauze envelope and refluxed in xylene. Untreated material was used as a control, to indicate when solvent extraction was complete. The weight of gel was determined by first weighing the gauze containing the gel, burning the gel in a blue Bunsen flame, and then reweighing the gauze.

2.9. Contact angle measurements

The degree of wetting between the reinforcement and matrix was examined by observing the shape and dimensions of a drop of liquid resin on a single filament. After mixing for 15 min, the filaments were dipped into the resin and suspended between two pieces of Plasticine on a glass slide. The drops were examined using an optical microscope. The contact angle could be either measured directly from a photograph or estimated using a computer program used in previous work [4, 9]. However, although the results are reproducible, precision is poor, with the scatter in θ being approximately $\pm 5°$.

These measurements were performed only on the coarser Spectra and Tekmilon fibres, with plasma-treated samples being exposed for 5 sec.

3. Results

3.1. Mechanical properties of composites

Table III shows the mechanical properties of the different UHMPE composites. The results for the ILSS show some significant distinctions between the different yarns. The untreated Celanese and Snia samples produced similar values (18 and 16 MPa, respectively),

TABLE III Mechanical properties of composites

	ILSS(MPa)	UFS(GPa)	FM(GPa)	TM(GPa)	TS(GPa)	CS(MPa)
Celanese						
Untreated	17	173	22	22	0.30	93
Plasma treated	29	162	20	21	0.31	97
Snia						
Untreated	16	172	27	31	0.47	88
Plasma treated	28	169	23	28	0.47	91
Spectra						
Untreated	8	142	68	41	0.62	79
Plasma treated	14	184	62	43	0.65	81
Tekmilon						
Untreated	23					
Plasma treated	29					
Unifos						
Untreated	6					
Plasma treated	9					

along with ~ 70% increase following 2 min plasma treatment of the reinforcement. Although a 70% increase was again achieved by plasma treatment, the ILSS of the Spectra composites was half that of the Snia. Untreated Tekmilon samples gave values of 23 MPa with an improvement of only 25% following pretreatment. The ILSS of composites prepared using the coarse Unifos monofilaments were 6 MPa before and 9 MPa after plasma treatment.

For a given volume fraction of fibres, the interfacial area between the reinforcement and matrix is inversely proportional to the filament diameter and, assuming equal levels of fibre/resin adhesion, the ILSS should display a similar dependence. Fig. 2, however, shows that this does not apply to the Tekmilon (diameter = 42 μm) which produced values considerably higher than the Spectra (36 μm) comparable with the much finer Celanese (16 μm) and Snia (18 μm).

Tekmilon also behaves differently when the ILSS is considered as a function of plasma treatment duration (Fig. 3). Whereas Snia and Spectra show a gradual increase, reaching a maximum after around 60 sec, Tekmilon shows the full improvement within 2 sec.

The UFS of the three composites tested were generally similar, though plasma treatment was found to produce an improvement in the Spectra, while giving

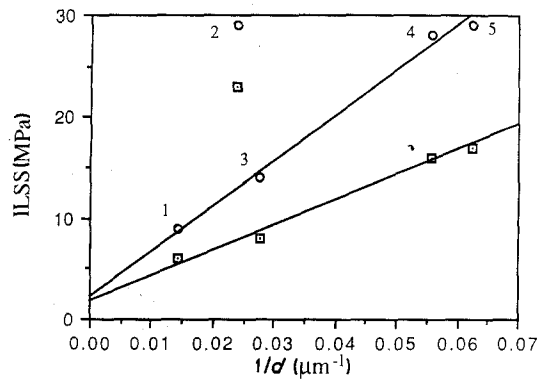

Figure 2 Plot of ILSS against inverse filament diameter. (1) Unifos (diameter = 70 μm), (2) Tekmilon (42 μm), (3) Spectra (36 μm), (4) Snia (18 μm), (5) Celanese (16 μm). (○) Plasma-treated, (□) untreated.

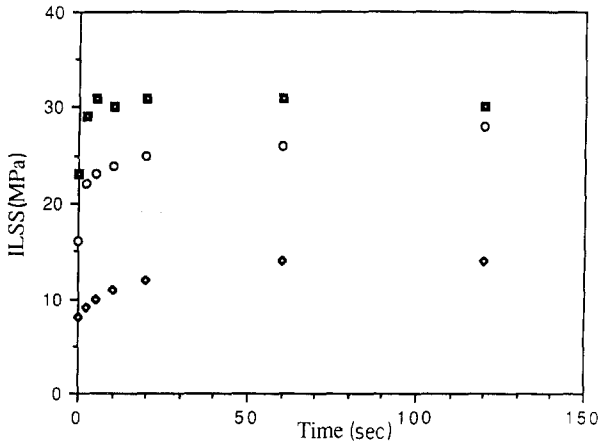

Figure 3 Plot of ILSS as a function of plasma treatment duration. (■) Tekmilon, (◇) Spectra, (○) Snia.

a slight reduction in the case of Celanese and Snia.

As expected, the high modulus, gel-spun Spectra produced composites of considerably higher TM and FM than the Celanese and Snia. Plasma treatment produced no significant change in stiffness.

When measuring the TS, the greater extension to failure of the reinforcement causes the resin matrix to crack early during testing, so that the load is supported solely by the fibres. The TS of the composites can therefore be related directly to fibre strength. The TS is unaffected by plasma treatment.

All the composites produced similar results for the CS with surface treatment having very little effect. The samples failed in shear, with a band appearing at 45° to the direction of compression, on the narrow face.

3.2. Gel content

Plasma treatment was found to produce a very small amount of cross-linking in each of the yarns. The increase in gel fraction in Spectra, with respect to plasma treatment duration, is shown in Fig. 4. It can be seen that the rate of formation reduces as time progresses, with cross-linking being complete after approximately 2 min. Fig. 5 shows gel content to be

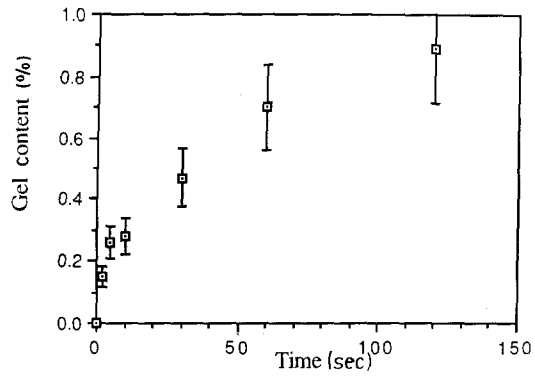

Figure 4 Gel content as a function of plasma treatment duration for Spectra.

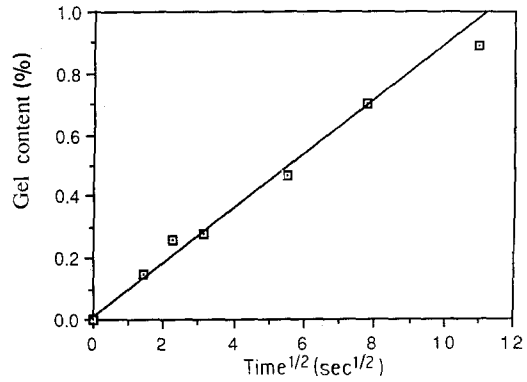

Figure 5 Gel content of plasma-treated Spectra plotted against the square root of treatment duration.

related to the square root of time. Due to the limited penetration of the oxygen plasma, gel is concentrated in the surface layers of the fibre, giving a cross-linked skin. The other three fibres produced insufficient gel for the mass to be determined as a function of time (due partly to oxidation of the stainless steel gauze), but a visual examination suggests that similar behaviour occurs. After 2 min the gel content was found to be ~0.3% in each case. The greater degree of cross-linking in Spectra is a result of its high molecular weight.

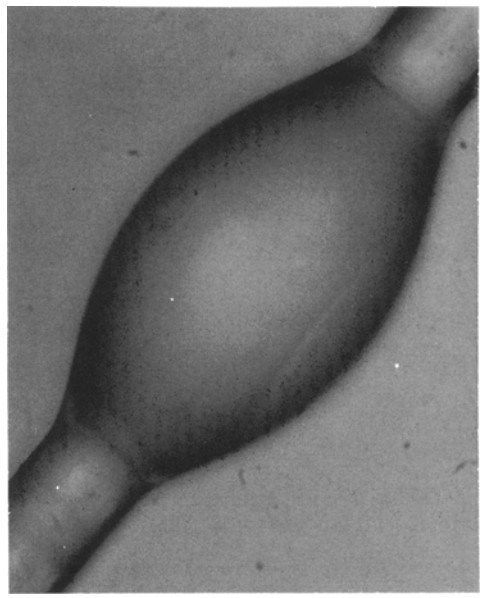

Figure 6 Drop of epoxy resin on a Spectra filament.

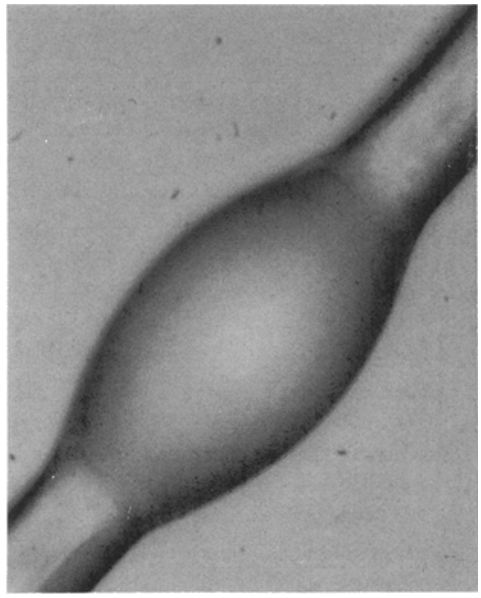

Figure 7 Drop of epoxy resin on a plasma-treated Spectra filament.

3.3. Contact angle measurements

The untreated Spectra and Tekmilon fibres displayed similar contact angles with epoxy resin, estimated to be 8° to 11°. Fig. 6 shows a single droplet on a Spectra filament, the distinct resin/fibre boundary showing clearly the extent to which the resin has spread. Following plasma treatment (Fig. 7), the contact angle was found to be reduced in each case to 3° to 5°. Improved wetting was also indicated by the absence of any clear demarcation between the fibre and resin.

3.4. SEM measurements

The very high draw ratios involved in producing UHMPE fibres, result in the formation of a fibrillar structure. This is shown by SEM as a series of longitudinal grooves on an otherwise smooth surface (Fig. 8). The nature of this structure varies between the different fibres, Spectra, for example, being much coarser (Fig. 9).

Exposure to oxygen plasma for 2 min results in extensive surface pitting. Fig. 10 shows the surface of a Tekmilon filament following plasma treatment and shows crack-like pits with a width of ~50 nm. Snia and Spectra show similar behaviour, though with Celanese pitting is on a much finer scale (Fig. 11).

Figs 12 and 13 show the grooves produced by dissolving the Celanese reinforcement from prepreg composites. In the case of the untreated yarn, the resin matrix clearly replicates the filament surface. However, the plasma-treated sample shows a cellular structure.

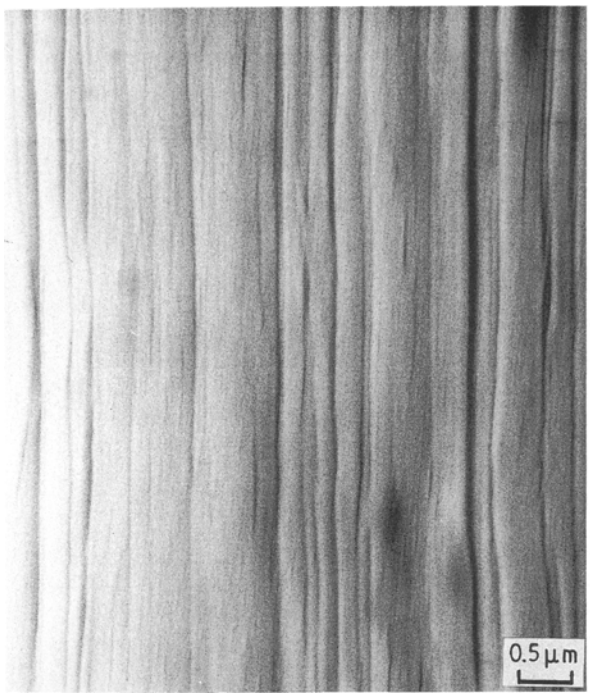

Figure 8 Scanning electron micrograph of untreated Snia filament.

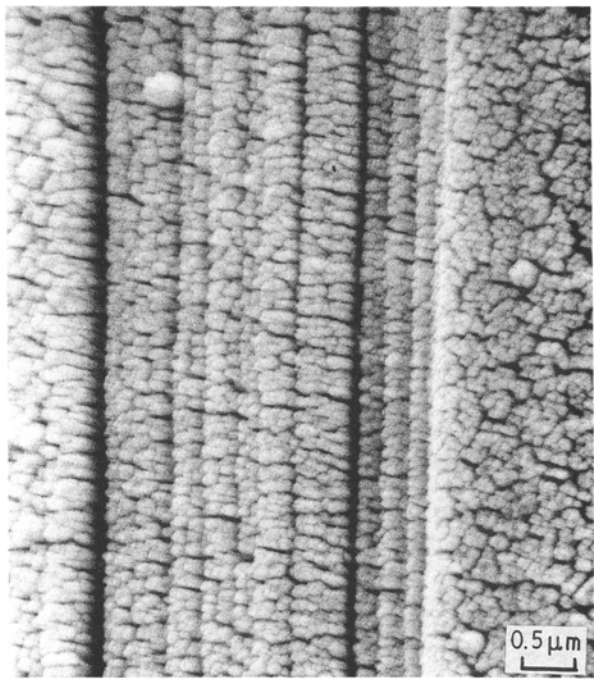

Figure 10 Scanning electron micrograph of plasma-treated (120 sec) Tekmilon filament.

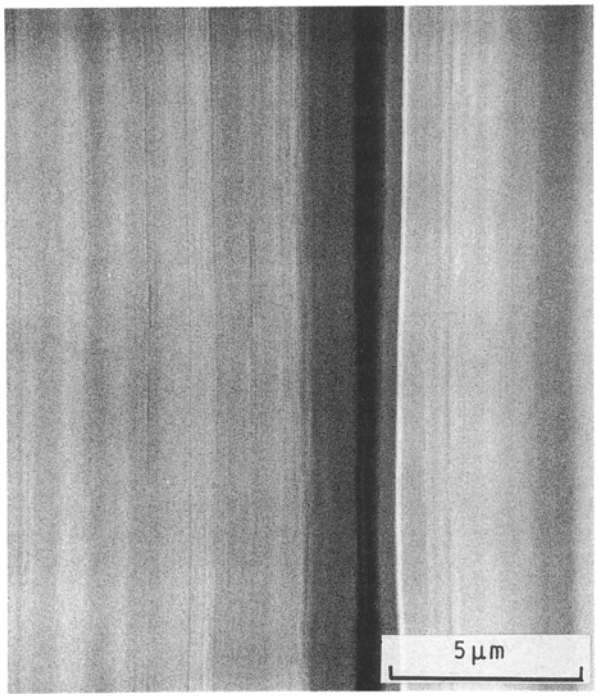

Figure 9 Scanning electron micrograph of untreated Spectra filament (note lower magnification).

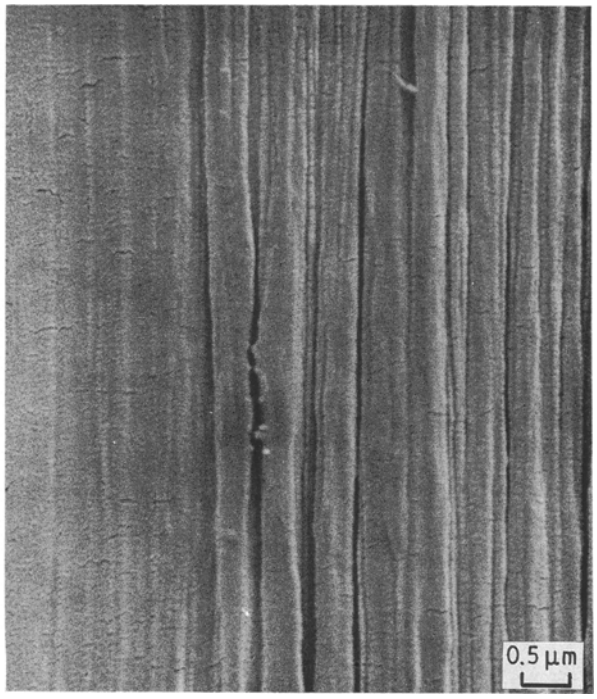

Figure 11 Scanning electron micrograph of plasma-treated (120 sec) Celanese filament.

4. Discussion

4.1. Adhesion and ILSS

Mechanical keying resulting from surface pitting has been proposed previously as a theory to explain the improved ILSS brought about by oxygen plasma treatment [3]. Fig. 10 shows the filament surface of Tekmilon yarn following plasma treatment and shows a large degree of micro-pitting. When compared with the smooth surface of the untreated fibre (Fig. 14), it can be seen how this would give a much greater potential bonding area. However, if wetting is incomplete and the pits are deep and narrow, the bonding surface may be lower than the untreated sample (Fig. 15) and, if this gives rise to voids, may lead to lower adhesion levels due to stress concentration.

To achieve good adhesion it is clearly necessary, though not always sufficient, to obtain extensive interfacial contact between the liquid resin and the fibres. In the case of polyethylene, wettability is low due to its inert, nonpolar surface. The contact angles measured

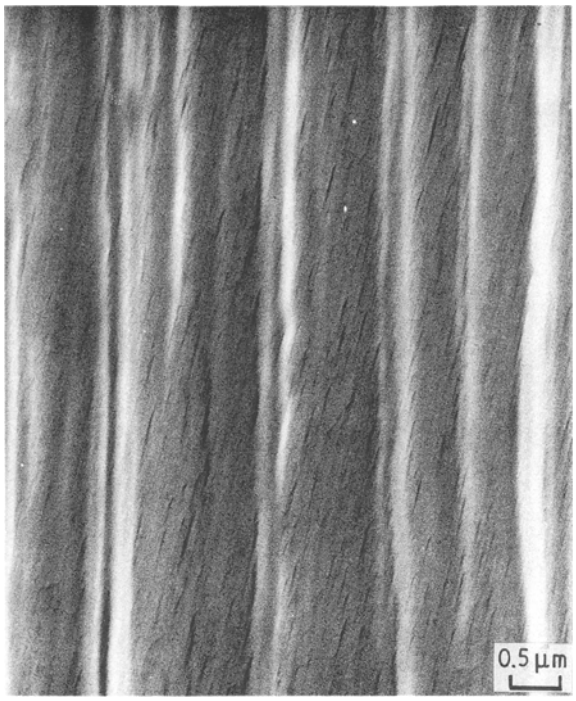

Figure 12 Scanning electron micrograph of groove resulting from the solvent extraction of untreated Celanese yarn from composites.

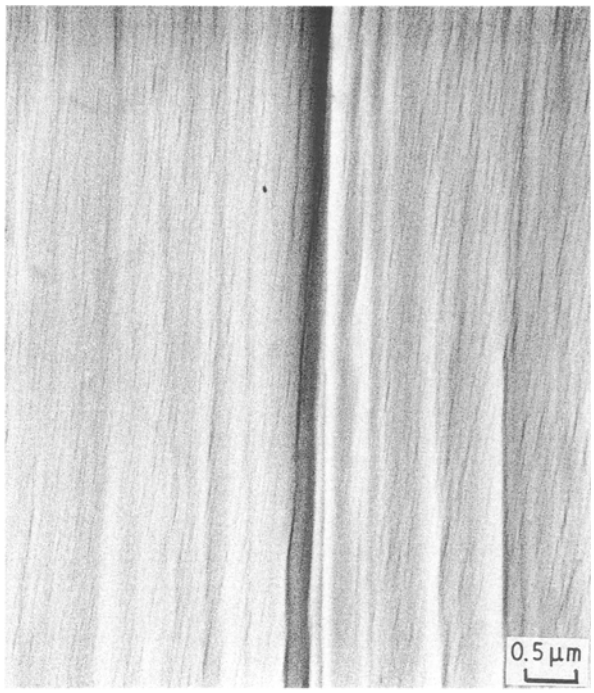

Figure 14 Scanning electron micrograph of untreated Tekmilon filament.

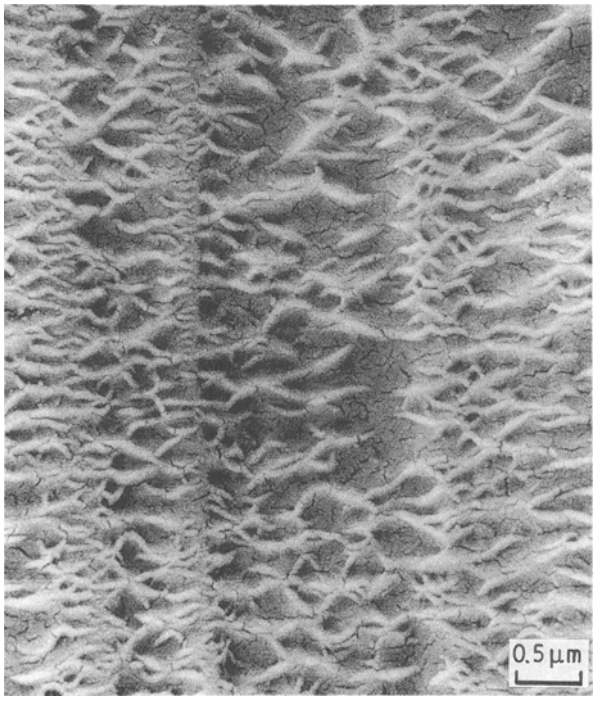

Figure 13 Scanning electron micrograph of groove resulting from the solvent extraction of plasma-treated Celanese yarn from composites.

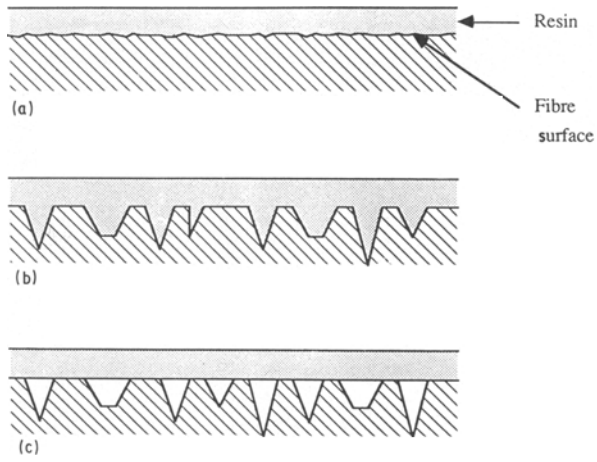

Figure 15 Schematic representation of how bonding area is affected by surface morphology and wetting. (a) Untreated fibre displaying a relatively smooth surface. (b) Plasma-treated fibre where deep pits provide a much increased bonding area. (c) Plasma-treated fibre where wetting is poor, leading to a reduced bonding area and possible stress concentrations.

from the untreated fibres were lower than is normally found for polyethylene, though this is in agreement with previous work which showed the surface energy of UHMPE fibres to increase with draw ratio [4]. The limited contact between the fibre and resin is best shown by Fig. 6, where a resin/filament boundary is clearly visible. This would suggest that, on a submicroscopic level at least, wetting was far from complete.

Pretreating the fibres with an oxygen plasma was found to cause a small reduction in θ and, perhaps more significantly, resulted in no clear demarcation between the fibre and resin (Fig. 7), indicating substantially improved contact.

Oxygen plasma contains a mixture of active oxygen species, mainly atomic oxygen with electronically and vibrationally excited atoms and ions. The initiation stage of the plasma/polyethylene reaction is the direct and rapid attack by atomic oxygen [10]

$$RH + O^{\bullet} \rightarrow R^{\bullet} + {}^{\bullet}OH \quad (4)$$

Oxidation proceeds via the following dominant

reactions

$$R^{\bullet} + O_2 \rightarrow ROO^{\bullet} \quad (5)$$

$$ROO^{\bullet} + R' \rightarrow ROOH + R'^{\bullet} \quad (6)$$

$$2ROOH \rightarrow R{=}O + H_2O + ROO^{\bullet} \quad (7)$$

$$ROOH \rightarrow RO^{\bullet} + OH^{\bullet} \quad (8)$$

$$RO^{\bullet} + R'H \rightarrow R^{\bullet} + R'OH \quad (9)$$

$$RH + OH^{\bullet} \rightarrow R^{\bullet} + H_2O \quad (10)$$

$$R^{\bullet} + O^{\bullet} \rightarrow RO^{\bullet} \quad (11)$$

The oxygen-containing groups produced on the polymer surface are capable of participating in relatively strong hydrogen-bonding interactions, which in turn lead to much improved wetting.

The surface reactions of polyethylene exposed to oxygen plasma have been studied [11] using an ESCA spectrometer. The concentrations of various oxygen containing groups are shown in Fig. 16 as a function exposure time. It can be seen that, with the exception of carbonate groups, a maximum is reached after approximately 5 sec. This makes an interesting comparison with the results for the ILSS, shown in Fig. 3 as a function of time. It can be seen that within 5 sec both the Snia and Tekmilon show dramatic increases of 44 and 35%, respectively. The Spectra composites show an increase of 25% which, although lower, is still significant. It can be concluded from these observations that the oxygen plasma produces an almost immediate increase in ILSS, due to the rapid oxidation of the fibre surface and subsequent improved wetting.

The degree of wetting necessary for satisfactory adhesion is unknown [12]. The overall interaction between the polyethylene fibres and the epoxy resin depends on the degree of contact achieved, and the magnitude of the molecular forces involved (dispersion, hydrogen-bonding etc.).

Although good wettability helps form a strong adhesive bond, it is not always sufficient due to poor surface (0.1 μm) cohesive properties [13, 14]. Most commercial polyethylenes contain a low molecular weight component which, despite being perfectly miscible in the molten polymer, is ejected to the surface during solidification. The high concentration of such material leads to a surface of low strength, commonly known as a weak boundary layer (WBL). A weak boundary layer may therefore be formed in UHMPE fibres during melt-spinning, and it is easy to envisage how a similar process could operate in the solidification/crystallization of the gel-spun spectra fibres. In the case of Spectra, another possible source of a WBL is the presence of any remaining solvent contaminating the fibre surface.

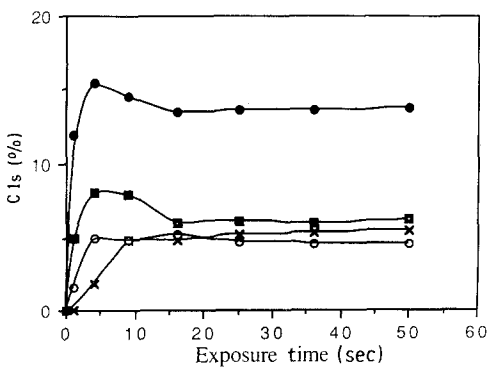

Figure 16 Intensity of various components of the C 1s spectrum of polyethylene in relation to C 1s(tot) plotted against time of exposure to oxygen plasma.

The effect of low molecular weight impurities and the presence of a WBL, has been demonstrated [13] by dissolving a commercial polyethylene in boiling xylene and precipitating the higher molecular weight polymer in acetone. When used as a melt adhesive, the purified polymer was found to give higher joint strengths than the raw material.

The adhesive properties of polyethylene have also been shown to improve following exposure to activated inert gases for short periods of time, in a technique known as CASING [15, 16]. It was thought that the metastable species of inert gas were responsible for an energy transfer between the plasma and polymer, forming polymer radicals and subsequent surface cross-linking, removing the WBL. The increase in gel mass was found to be proportional to the square-root of exposure duration, which was a general observation for all noble gas, hydrogen and nitrogen plasmas. This suggested that the diffusion of plasma gas atoms into the polymer was responsible for the increase in thickness of the cross-linked skin. However, the diffusion coefficients estimated from these results were very much lower than measured values for light gas atoms in polyethylene. Because of this it was suggested that the ultra-violet radiation emitted by the plasma was responsible for inducing cross-linking [17]. Subsequent work has shown that this is the case [18], the effective wavelengths being less than 190 nm. The gel mass (square root) time dependence and depth of penetration can be fully accounted for in terms of the attenuated light model and the polychromatic nature of plasma ultraviolet radiation.

Oxygen plasma generally causes a reduction in the molecular weight of polyethylene [10]. The plasma produces ultraviolet radiation which penetrates into the polymer producing free-radicals, the concentration of which decays exponentially with depth of penetration, in accordance with Beer's law. Oxygen atoms are able to diffuse readily into polyethylene forming a concentration gradient which is lower than that of the polymer radicals. Consequently cross-linking can only occur where ultraviolet intensity is great, giving a high polymer radical to oxygen ratio. For penetrations where the intensity is low, oxygen atoms mop up polymer radicals preventing rebonding. It was suggested that treating polyethylene with oxygen plasma would produce a very thin cross-linked skin (typically 50 nm), below which a reduction in molecular weight would occur due to the predominance of polymer radical oxidation. This would not cause the WBL to be removed.

If this were the case, it is clear that gel content would quickly reach a maximum and would not be a function of time. The results for the gel fraction of

spectra (Fig. 4) show that this is not so. Instead, cross-linking still appears to be occurring after 2 min and would result in a cross-linked skin of $>0.5\,\mu m$, sufficient to remove any WBL. Fig. 5 also shows that gel content is related to the square root of time, in common with inert gas plasmas. The other three yarns appear to display similar behaviour, although the lower gel content would form a skin of 0.2 to 0.3 μm (compared with an estimated WBL thickness of 0.1 μm).

The unexpected ability of the oxygen plasma to produce significant cross-linking in UHMPE fibres can be explained in terms of a number of factors:

(i) The relatively high power of the discharge (120 W compared with a maximum of 60 W in previous work) would produce ultraviolet radiation of greater intensity, increasing polymer radical concentration;

(ii) the higher power allows treatment times to be significantly reduced, limiting the depth to which oxygen atoms are able to penetrate;

(iii) orientation of polyethylene has been shown to reduce its permeability to gases [19].

The three effects combine to increase the polymer radical/oxygen ratio throughout the surface layers of the fibres, allowing sufficient cross-linking to, at least partially, remove the WBL.

Further evidence for the presence of cross-linking is provided by the grooves resulting from the solvent extraction of the fibres from the Celanese prepreg composites. The cellular structure observed in the plasma-treated sample (Fig. 13), although previously thought to be a replica of the pitted fibre surface, seems more likely to be undissolved, cross-linked residue from the fibre itself.

The effect of surface cross-linking on the ILSS is shown in Fig. 3. Following the initial increase due to improved wetting, the ILSS of the Snia and Spectra composites gradually increase as the WBL is progressively removed. The ILSS of the Tekmilon samples, however, shows no increase after the first 5 sec exposure suggesting that no WBL is present. The reason for this is not known, though it may be due to specific processing routes. It seems likely that the drawing of the fibres in *n*-decane at 130 °C would result in the surface layers being dissolved.

The absence of a WBL also explains the higher than expected ILSS obtained using the untreated yarn. Fig. 2 shows that, with the exception of the Tekmilon, the ILSS is inversely proportional to the filament diameter and therefore proportional to the resin/fibre interfacial area. The values obtained for the Tekmilon composites (also shown in Fig. 2) suggest that, with no WBL present, superior levels of fibre/resin adhesion were achieved, giving a higher ILSS than predicted from the filament diameter.

As mentioned above, the ILSS of Tekmilon composites increases to a maximum within 5 sec of plasma treatment, due to rapid surface oxidation. SEM of the fibre surface in Fig. 17 shows that no pitting has occurred in that time and although prolonged exposure does produce pits (Fig. 10), these do not improve

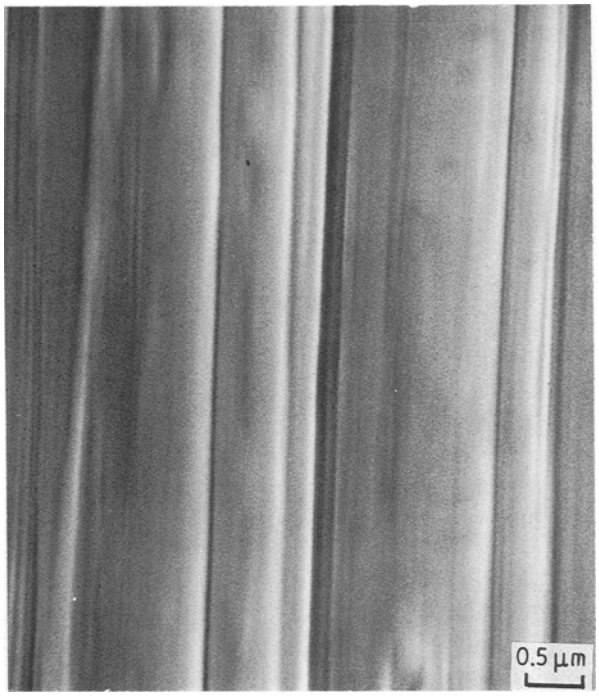

Figure 17 Scanning electron micrograph of plasma-treated (5 sec) Tekmilon filament.

adhesion and may be detrimental. Surface pitting may have a slight effect in the case of the other fibres. Fig. 3 shows that values for the ILSS are still increasing after 60 sec. However, tests on the pull-out strength of UHMPE monofilaments embedded in epoxy resin [20] have shown that, following oxygen plasma treatment, failure occurs not at the fibre/resin interface, but by shear within the fibre itself. This suggests that the combination of improved wetting and surface cross-linking is sufficient to raise the interfacial bond strength to a level greater than the shear strength of the fibre, so that the pits have no effect.

4.2. Tensile modulus and flexural modulus

The rule of mixtures can be used to predict the theoretical TM of the composites. Neglecting any void content we have

$$(TM)_c = E_f V_f + E_r(1 - V_f) \qquad (12)$$

where $(TM)_c$ is the calculated TM of the composite, E_f and E_r are the respective TM of the fibres and resin, and V_f is the fibre volume fraction. Given that the composites have a nominal V_f of 0.55, and the resin has a relatively low TM, the expected values for the Celanese, Snia and Spectra composites are 24, 32 and 46 GPa, respectively. The experimental results (22, 31 and 41 GPa) show a reasonable agreement with theory, the difference probably as a consequence of some fibre misalignment. In the case of the Celanese and Snia composites, the TM and FM are very similar, though Spectra is shown to be much stiffer flexurally (68 GPa).

Both the TM and FM are measured at very low strains and as a result, it is unlikely that any failure

will occur within the sample. This is shown experimentally in that increased fibre/resin adhesion has no significant effect on the values obtained.

4.3. Tensile strength and compressive strength

The tensile strength of the composites can also be predicted using the law of mixtures. We have

$$TS = \sigma_f V_f + \sigma_f(1 - V_f) \quad (13)$$

where TS is the tensile stress on the composite parallel to the fibre direction, and σ_f and σ_r are the stresses on the fibres and resin matrix, respectively, but due to the greater extension to failure of the fibre reinforcement, the formula can be modified to give

$$(TS)_c = \sigma_f V_f \quad (14)$$

Given a nominal fibre volume fraction of 0.55, the expected values for the TS of the Celanese, Snia and Spectra composites would be 0.46, 0.66 and 1.2 GPa, respectively. Table III shows the experimental results (0.30, 0.47 and 0.62 GPa) to be considerably lower than predicted. This may be due to poor fibre alignment giving an uneven distribution of stress between the reinforcement. As the TS of UHMPE composites is dependent purely on the properties of the fibres, improved adhesion due to plasma treatment had no effect.

Although the TS determined by these measurements corresponds to fibre fracture, actual composite failure occurs at a much lower stress due to resin cracking. While the composites were still able to support a load applied parallel to the direction of reinforcement, the flexural strength would have been much reduced. The high extension to failure of UHMPE fibres means that the ultimate failure of composites may, in many practical situations, be determined by the properties of the resin, rather than the reinforcement.

Owing to the poor compressive behaviour of UHMPE fibres, the CS of the composites is dependent primarily to the resin matrix. As expected, all the composites give similar values (80 to 90 MPa) and, with the nominal volume fraction of the resin being 0.45, and the compressive strength 120 MPa, these are not unreasonable. Plasma treatment was found to produce a minor improvement, probably due to increased resistance to resin cracking.

4.4. Ultimate flexural strength

As all the samples tested produced fairly similar results for the UFS, it seems that this is dependent mainly on the matrix. Flexing appears to cause failure due purely to resin cracking, breaking down the composite. Examining the samples after testing shows the fibres to be intact. Plasma treatment reduces the degree of damage in the matrix, the higher adhesion increasing the constraint applied by the reinforcement. Because of this it would be expected that pretreatment would improve the UFS, though the experimental results (Table III) show that this is not the case. An improvement is seen with the Spectra composites which is probably due to the very low ILSS of the untreated fibre.

5. Conclusions

The interlaminar shear strength of UHMPE composites is considerably improved by pretreating the reinforcement with an oxygen plasma. By careful selection of the treatment conditions, it is possible to obtain the maximum increase in fibre/resin adhesion with no significant reduction in the bulk properties of the fibre.

The oxygen plasma acts by rapidly oxidizing the polymer surface, increasing the surface energy and therefore improving fibre/resin contact. The plasma ultraviolet radiation is able to cross-link the surface layers of the fibres to produce a skin of sufficient thickness to remove the weak boundary layer. The poor adhesive properties of polyolefines are commonly associated with the presence of a WBL. Pretreatment with an oxygen plasma also produces extensive pitting of the filament surface, although the effectiveness of this in improving adhesion is not clear, as failure in treated composites occurs not at the interface, but by shear within the fibre itself.

The interlaminar shear strength of the composites is also dependent on the filament diameter, finer fibres providing a greater bonding area between the reinforcement and matrix.

The tensile and flexural moduli and tensile strength of UHMPE composites can be directly related to the fibre properties by the law of mixtures. The relatively low stiffness of the resin means that the modulus of the composite is simply the fibre volume fraction multiplied by the modulus of the fibre. Owing to the greater extension to failure of the fibres when compared to the resin, the tensile strength of the composites is determined purely by the fibres. It should be noted, however, that in most practical situations, composite failure would occur at the onset of resin cracking.

The ultimate flexural strength and the compressive strength are dependent mainly on the properties of the matrix. Failure during bending is a result of extensive resin cracking in the loaded region of the sample, the reinforcement remaining undamaged. Owing to the low compressive strength of UHMPE fibres, loading the composites in compression causes the load to be borne primarily by the matrix. The compressive strength of the composites is therefore largely independent of fibre properties and similar for all the different samples tested.

Although improving the interlaminar shear strength significantly, pretreating the reinforcement with oxygen plasma was found to have only a minor effect on the other properties of the composites.

Future work will be concerned with the unusual impact properties exhibited by UHMPE composites.

References

1. G. CAPACCIO and I. M. WARD, *Nature Phys. Sci.* **243** (130) (1973) 143.

2. P. SMITH and P. J. LEMSTRA, *J. Mater. Sci.* **15** (1980) 505.
3. N. H. LADIZESKY and I. M. WARD, *Comp. Sci. Technol.* **26** (1986) 129.
4. M. NADIN and I. M. WARD, *Mater. Sci. Technol.* **3** (1987) 814.
5. G. CAPACCIO, T. A. CROMPTON and I. M. WARD, *J. Polym. Sci. Polym. Preprints* **14** (1976) 1641.
6. *Idem, ibid.* **18** (1980) 301.
7. European Pat. Appl. 0168923 (filed 15 May 1985).
8. J. B. STURGEON, "Specimens and Test Methods for Carbon Fibre Composites" Royal Aircraft establishment, UK TR71026 (1971).
9. J. I. YAMAKI and Y. KATAYAMA, *J. Appl. Polym. Sci.* **19** (1975) 2897.
10. M. HUDIS, in "Techniques and Applications of Plasma Chemistry", edited by J. R. Hollahan and A. T. Bell (Wiley, London, 1974) p. 113.
11. D. T. CLARKE and A. DILKS, *J. Polym. Sci. Polym. Comp.* **17** (1979) 7.
12. D. M. BREWIS and D. BRIGGS, *Polymer* **22** (1981) 23.
13. J. J. BIKERMANN, *Adhes. Age* **2** (3) (1959) 23.
14. *Idem*, in "The Science of Adhesive Joints" (Academic Press, New York, 1968) p. 164.
15. R. H. HANSEN and H. SCHONHORN, *J. Polym. Sci. B* **4** (1966) 203.
16. H. SCHONHORN and R. H. HANSEN, *J. Appl. Polym. Sci.* **11** (1967) 1461.
17. M. HUDIS and L. E. PRESCOTT, *J. Polym. Sci. B* **10** (1972) 179.
18. M. HUDIS, *J. Appl. Polym. Sci.* **16** (1972) 2397.
19. P. S. HOLDEN, G. A. ORCHARD and I. M. WARD, *J. Polym. Sci. Polym. Phys. Edu.* **23** (1985) 709.
20. N. H. LADIZESKY and I. M. WARD, *J. Mater. Sci.* **18** (1983) 533.

Received 31 October
and accepted 8 November 1989